Physically Meaningful Modeling of the 3-Zone and 4-Zone Simulated Moving Bed Processes

G. Hotier
Institut Français du Petrole, 92502 Rueil-Malmaison, France

This article is intended as a complement to a recent article in this journal, "Comparative Study of Flow Schemes for a Simulated Countercurrent Adsorption Separation Process" by Ching et al. (1992). These authors carried out experiments on continuous separation of three carbohydrate mixtures with both the usual four-section scheme and a three-section scheme: fructose dextran (MW ≅ 9,400), raffinose dextran (MW = 6,000), and fructose-raffinose. These two schemes were modeled as equivalent true countercurrent systems. From the experiments and model results they conclude that the equivalent true countercurrent model is fully adapted to represent the four-section scheme, but a major discrepancy arises with the three-section scheme: the raffinate concentration is not correctly predicted.

From these results it may be concluded that when a physically meaningful modeling of the equivalent true countercurrent is realized, the apparent discrepancy disappears. From another standpoint, such a mismatch between the experiments and model predictions would not have been observed with a model that considers the periodic port motion. Such a model foresees a cyclic steady state where extract and raffinate compositions vary throughout the period T; they can be considered as constant only when averaged over the period. It is worth comparing the results of these two models, especially when the equivalent countercurrent representation is not very close to the physical phenomenon it should represent.

We agree with their major finding that a three-zone scheme represents necessarily a higher desorbent demand than a four-zone scheme.

Introduction

From the modeling point of view, batch chromatography and continuous chromatography are not as different as they are in practice. Nevertheless, all the conceptual work that leads from a single-column chromatographic separator to a simulated countercurrent (SCC) process has to be performed. Broughton et al. (1970) first published an article on this subject. Since then modeling of the SCC separation process has received considerable attention in the literature. In recent years, most of the articles on the subject are applied to three- or four-section simulated moving beds. The main teams that have contributed on the subject are Barker et al. (1983), Ching and Ruthven (1985a,b), Ching et al. (1985, 1987, 1988), Hashimoto et al. (1987), Morbidelli et al. (1991), and Ruthven and Ching (1989).

The different approaches that have been followed may be classified into two main types:

1. Simulated moving-bed modeling, based on an equivalent real countercurrent system.
2. The modeling of the simulated moving bed takes into consideration the periodical switching of the inlet and outlet ports.

In type 1 models, the fluid-flow rates in the real countercurrent operation are equivalent to those in the simulated moving bed, but the "fixed" solid phase is moved countercurrently with a speed calculated in accordance with the switching period and the column length. Each of these two types of models can be combined with either a discontinuous representation of the separation column (theoretical stage model with balance equations on each stage) or with a continuous one (continuous flow model with partial differential equations over the entire column).

This finally gives four modeling patterns of the simulated moving bed, as suggested by Ruthven and Ching (1989):

I(a). Equivalent real countercurrent with a discontinuous representation (theoretical trays) of the separation column.

I(b). Equivalent real countercurrent with a continuous representation (partial differential equations) of the separation column.

II(a). Periodical port motion model with a theoretical stage representation of the separation column.

II(b). Periodical port motion model with continuous representation (partial differential equations) of the separation column.

For each of these four patterns, different models are available in the literature. The differences between these models are that they take account of some physical phenomena that may occur in the adsorption column: axial dispersion, mass-transfer resistance, diffusion in the porosity of the adsorbent. The equilibrium laws between fluid phase and solid phase (adsorbent) and the numerical resolution methods are different from one model to another. Some of the models have been validated by experimental measurements on simulated moving-bed units for a given separation, but it is not a general rule.

For sugar separations and especially for glucose–fructose separation on ion-exchange resins, many models have been proposed. At least one model is available for each of the four modeling patterns described previously. The models are very often validated by experimental measurements on a simulated moving-bed unit. Generally, the authors show a comparison between model predictions and experimental results. They describe the steady-state concentration profile in the different sections of the simulated moving bed (Ching and Ruthven, 1985a; Ching et al., 1985, 1987; Hidajat and Ching, 1990), and even the concentration evolution during the transient regime can be found (Ching and Ruthven, 1985b). Except for a few of them (Barker and Ganetsos, 1989), most of the experimental results are given for dilute sugar concentrations; the equilibrium isotherms are then often linear and the modeling is easier.

Ching and his coworkers (1988) present a study of monoethanolamin-ethanol separation on ion-exchange resins; they show comparisons between the type I(a) model predictions and experimental measurements on a simulated moving-bed unit. Barker et al. (1983) have developed a type II(a) model for dextran fractionation on porous silica and validated it with experimental results. Liappis and Rippin (1979) have developed two different models [types I(b) and II(b)] to study butanol-2-*t*-amylalcohol separation; they present theoretical profiles obtained with the models but no experimental measurements to validate them. On the other hand, Hashimoto et al. (1987) validated a type I(b) model with experimental results on glucose–NaCl separation.

Other contributors working in the field of hydrocarbons (Morbidelli et al., 1991; Storti et al., 1989a, 1992b; Storti et al., 1988a,b; Balannec and Hotier, 1992) or of fine chemicals (Nicoud and Bailly, 1992) have developed models according to the four patterns. Even if the major part of these modelings have been made in the case of the four-zone simulated moving-bed schemes, it has been shown that models a and b yield exactly the same results for batch chromatography, and in practice models I and II are equivalent provided that a certain number of conditions, for example, a minimum number of ports, are fulfilled.

Table 1. Fructose–Dextran T9 Separation Experiments

	Flow Scheme	Four Section	Three Section
	Feed, F (cm^3/min)	2.0	2.0
	Solid, S (cm^3/min)	4.1	4.1
	Eluent, D (cm^3/min)	3.1	3.1
	Extract, E (cm^3/min)	2.5	2.5
	Raffinate, R (cm^3/min)	2.1	2.6
	Actual eluent† (cm^3/min)	6.5	6.5
	Switch time‡ (min)	9.8	9.8
Extract§	Concentration (% w/v)	Fr = 4.06 T9 = 0.10	Fr = 4.05 T9 = 0.0
	Purity	0.98	1.00
	Recovery	1.00	1.00
	Concentration ratio	0.81	0.81
Raffinate$^{\#}$	Concentration (% w/v)	Fr = 0.00 T9 = 4.58	Fr = 0.00 T9 = 1.68
	Purity	1.00	1.00
	Recovery	0.96	1.00
	Concentration ratio	0.92	0.34

Source: Reproduced from *AIChE J*, **38**, 1744 (1992).

[*] This table displays (1) elements coming from simulated moving bed experimental operating flow rates and other elements used in the equivalent true countercurrent model, and (2) material balances.

[†] Actual eluent $= [(\epsilon/1-\epsilon)]S + D$, where $\epsilon = 0.45$.

[‡] Switch time $= [(1-\epsilon)aL]/S$, where $a = 1.54$ cm^2 and $L = 47.5$ cm.

[§] Extract purity is defined as $c_i/(c_i + c_j)$ where i is the more strongly adsorbed species and j is the less strongly adsorbed species. Extract recovery is defined as the ratio of the amount of i recovered in the extract to the initial amount of i in feed. Extract concentration ratio is defined as the ratio of concentration of i in the extract to the initial concentration of i in feed.

[#] Raffinate purity is defined as $c_j/(c_i + c_j)$ where i is the more strongly adsorbed species and j is the less strongly adsorbed species. Raffinate recovery is defined as the ratio of the amount of j recovered in the raffinate to the initial amount of j in feed. Raffinate concentration ratio is defined as the ratio of concentration of j in the raffinate to the initial concentration of j in feed.

Experimental Results

Although there is no theoretical reason why a model that gives accurate and precise representation of a four-zone scheme could not represent a three-zone scheme, there must be practical reasons. So let us examine the data and material balances for the fructose–dextran separation for both the three-zone and the four-zone schemes as displayed in Table 1, reproduced from Ching et al.'s article (the two other examples will be shown in Tables A1 and A2).

Let us assume for the sake of simplicity that all the solutions exhibit a common density of 1 g/cm^3, and let us try to derive component by component what are the net fluxes entering or leaving the unit once the steady state has been reached (see Table 2).

Obviously there is a problem with the dextran material balance in the three-section scheme. As the unit has reached the steady state (and as it can be checked in Table 1), the recovery of dextran is 100%, the final concentration of dextran is 1.68 wt/v % in raffinate and 0 in extract. Thus the raffinate flow rate can be recalculated as

Table 2. Complete Material Balance in the 3-Zone Experiment*

Flow scheme	Four Section	Three Section
Fructose in (% Fructose in Feed × F)	5 wt/v % × 2 cm^3/min = 0.1 g/min	5 wt/v% × 2 cm^3/min = 0.1 g/min
Dextran T9 in (% Dextran in Feed × F)	5 wt/v% × 2 cm^3/min = 0.1 g/min	5 wt/v% × 2 cm^3/min = 0.1 g/min
Fructose out*	4.06 wt/v% × 2.5 cm^3/min + 0 = 0.1015 g/min	4.05 wt/v% × 2.5 cm^3/min + 0 = 0.10125 g/min
Dextran T9 out†	0.1 wt/v × 2.5 + 4.58 wt/v × 2.1 cm^3/min = 0.09868 g/min	1.68 wt/v% × 2.6 cm^3/min = 0.04368 g/min
Fructose out/in	1.015	1.0125
Dextran out/in	0.9868	0.4368

*A false raffinate flow rate comes out because of mixing actual and derived values.
**% Fructose in extract × E + % Fructose in raffinate × R.
†% Dextran in extract × E + % Dextran in raffinate × R.

$$R = \frac{5 \text{ wt/v } \% \times 2 \text{ cm}^3/\text{min}}{1.68 \text{ wt/v } \%} = 5.95 \text{ cm}^3/\text{min}.$$

On this basis, it becomes apparent that Table 1 mixes actual flow rates and derived flow rates related to the equivalent true countercurrent model that is supposed to represent the unit. Thus it seems useful to show both the actual flow rates and the derived ones (Table 3).

It is not our purpose to argue if the derived values that must be considered in zone I is 3.15 or 3.1 cm^3/min, but when starting from actual values, that is, actual desorbent 6.5 cm^3/min, $T = 9.8$ min, $\epsilon = 0.45$, $a = 1.54$ cm^2, and $L = 47.5$ cm, values of D and S are, respectively, 3.15 cm^3/min and 4.1 cm^3/min. This difference may come from losses in the three-section experiment or from a slight inaccuracy in the flow rate measurements, or from a slight inaccuracy in the T9 concentration measurements.

Discussion

Our concern in this article is to point out that the actual and the derived material balances for the three-section scheme are not identical. Therefore, as the derived flow rates are not representative of the actual flow rates in the unit, there must be discrepancies.

The simple idea that leads to that erroneous mass balance in the three-section scheme is to deduce Figure 1b from Figure 1a. This has been shown to be valid in the four-section scheme (Figure 1a) but false in the three-section scheme (Figure 1b). Actually, there is no paradox: the "return" branch of the solid circulation was omitted in the three-section scheme; by including it, we obtain Figure 1c.

Table 3. Actual Experimental Simulated Moving Bed and Derived Flow Rates Considered by Ching et al. for the Equivalent True Countercurrent Model*

	Four Section		Three Section	
Flow Scheme	Actual	Derived	Actual	Derived
Zone I (cm^3/min)	6.5	3.15	6.5	3.15
Zone II (cm^3/min)	4.0	0.65	4.0	0.65
Zone III (cm^3/min)	6.0	2.65	6.0	2.65
Zone IV (cm^3/min)	3.9	0.55	—	—
Makeup desorbent (cm^3/min)	2.6	2.6	6.5	3.15
Feed (cm^3/min)	2.0	2.0	2.0	2.0
Extract (cm^3/min)	2.5	2.5	2.5	2.5
Raffinate (cm^3/min)	2.1	2.1	5.95	2.6
Switch time/min	9.8	9.8	9.8	9.8
Losses (cm^3/min)	—	—	0.05	0.05

*Fructose 5%; dextran T9 5%.

A physically meaningful modelization (according to the true countercurrent pattern) equivalent to the actual unit must take into account this "parallel branch." Part of the eluent is diverted down to the raffinate outlet, where it creates undesired but unavoidable dilution. Thus the equivalent true countercurrent is a valid representation of the actual units, whatever the flow scheme, if every flow is carefully taken into account. For example, the other three-zone schemes may be modeled by Figure 1d.

It may be seen that rather than using parameters in Figures 1a, 1b, 1c and 1d, numerical values from Table 3 have been employed, in order to show a practical case.

The considerable experimental work done by Barker and coworkers with this system is reported to be correctly predicted by the true countercurrent pattern modeling. Since they do not report that they have to account for any additional dilution both for the extract and the raffinate, it may be supposed that they consider this dilution as obvious from the material balances standpoint.

When Barker and coworkers' article (1992) is further examined, they claim that the three-zone scheme can achieve similar concentrations and reduce the mobile phase requirements to comparable levels (with reference to the four-zone scheme) by employing the product splitting and recycling technique. This suggestion is relevant in practice, but the true countercurrent modeling will no longer be employed.

Let us now think of what will give a model that takes account of the actual port motions. For both three- and four-zone schemes the model converges toward a cyclic steady state. This means that when convergence is reached, the extract and the raffinate compositions are constant only when averaged over the switching period. On the contrary, instant compositions vary in large proportions.

Four-zone case

The extract and raffinate instant compositions vs. time curves (Figure 2d and Figure 2e) are of course tied to the concentration profiles (Figures 2a, 2b and 2c). Conclusions that might be drawn for the four-zone case follow:

1. When the flow rates are correct in zones I and IV, it may be seen that pure solvent is exchanged between columns

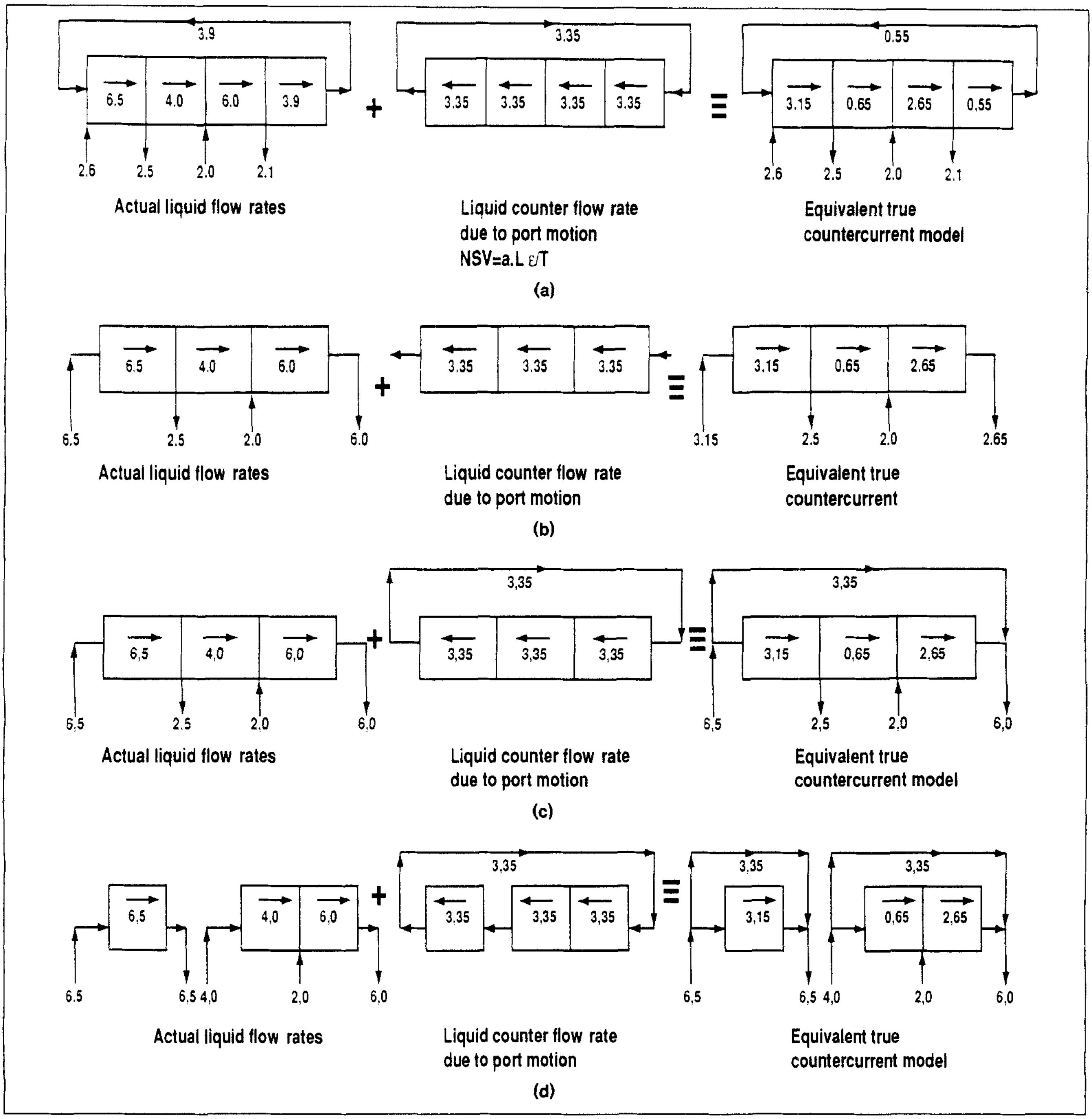

Figure 1. Equivalent true countercurrent processes.

(a) 4-zone, valid conceptual representation. (b) 3-zone, false conceptual representation. (c) 3-zone, valid conceptual representation. (d) 3-zone with separate desorption zone, valid conceptual representation.

C_8 and C_1, thus minimizing the solvent makeup *D*. In this respect, zone IV should not be a "buffer zone," as it may be read in UOP's literature, but rather a "solvent saver zone".

2. The front and back ends of both peaks *A* and *B* are translated at a *single constant speed* throughout the system. The edges of the peaks are nearly constant in shape throughout the switching period.
3. It has been shown that when comparing the result of a simulation done with the equivalent real countercurrent, with experimental results or with the results of a simulation taking into account port motion, the best agreement is reached when the concentration profile is measured at $t = T/2$ (Figure 2b).

Three zone case

The extract instant composition vs. time is exactly the same as in the four-zone scheme (not represented). This is not the case for the raffinate instant composition. Let us examine

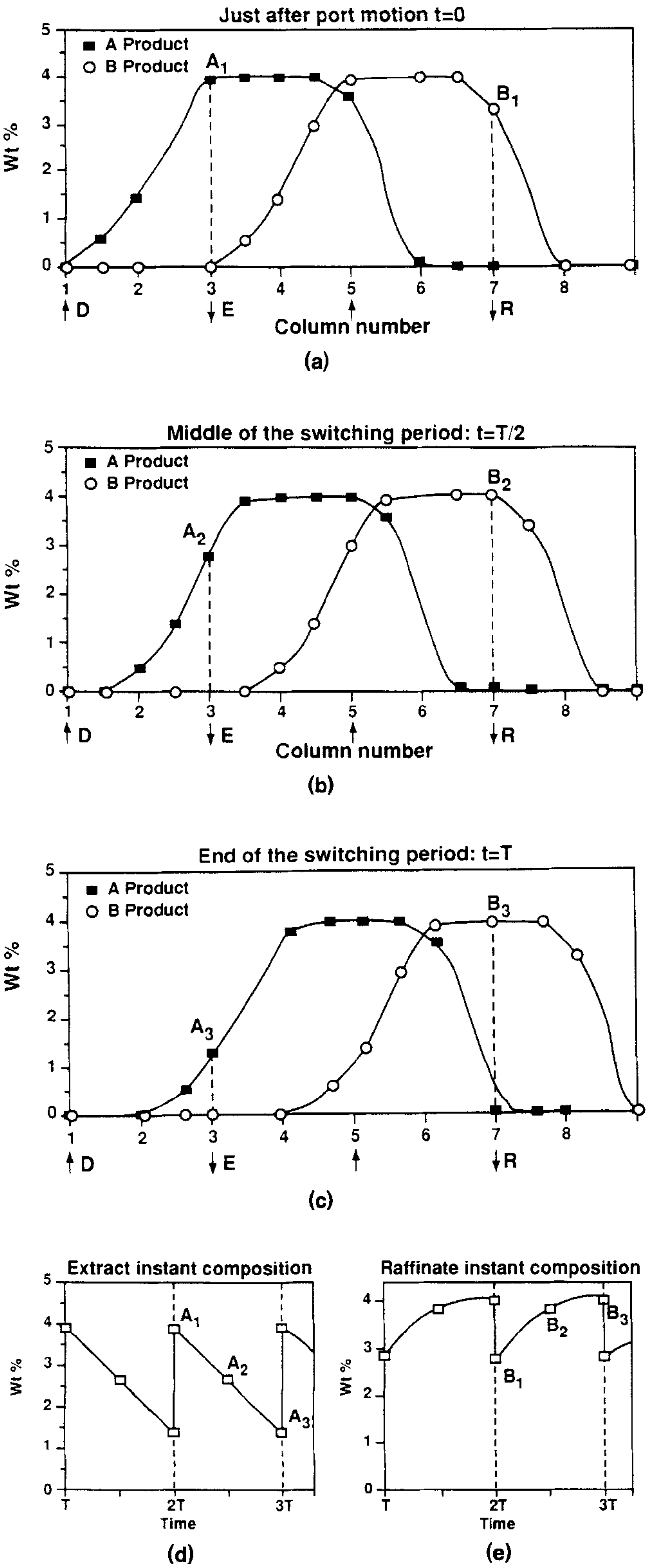

Figure 2. Concentration at different times in the case of 4-zone simulated moving bed.

(a) Concentration vs. axial position in adsorber just after port motion. (b) Concentration vs. axial position in adsorber at the middle of the switching period. (c) Concentration vs. axial position in adsorber at the end of the switching period. (d), (e) Concentration vs. time for the raffinate and the extract.

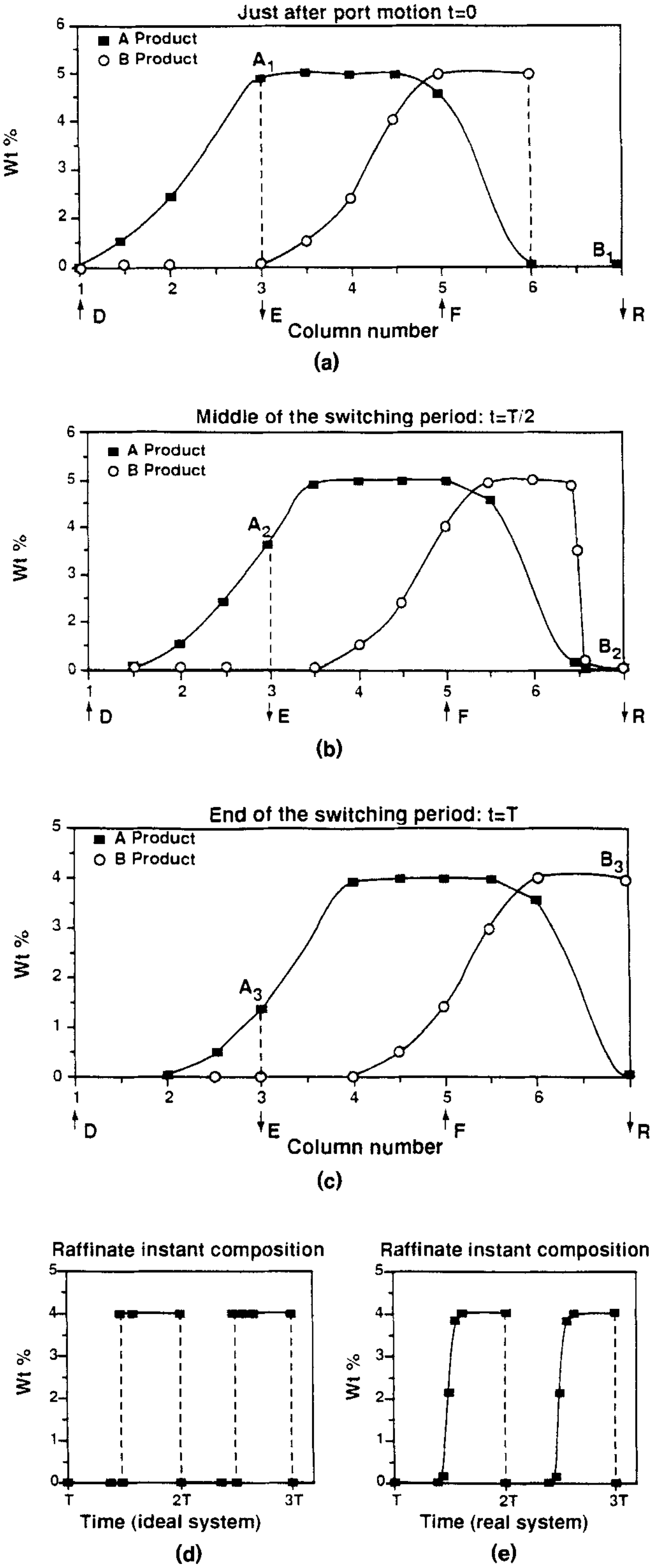

Figure 3. Concentration at different times in the case of 3-zone simulated moving bed.

(a) Concentration vs. axial position in adsorber just after port motion. (b) Concentration vs. axial position in adsorber at the middle of the switching period. (c) Concentration profiles vs. axial position in adsorber at the end of the switching period. (d), (e) Concentration vs. time for the raffinate (ideal and real system).

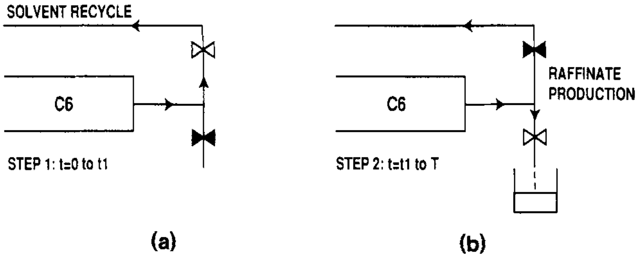

Figure 4. Product splitting system to reduce desorbent requirement.

(a) Switching period first step: desorbent recycle. (b) Switching period second step: raffinate production.

concentration profiles (Figures 3a, 3b and 3c). The conclusions that might be drawn from the three-zone case are:

1. However close to the optimal ones, flow rates in zone I and in zone III are such that pure solvent exchange is not feasible between column C_1 and C_6. If pure plug flow and instant equilibrium were reached, the raffinate instant composition represented in Figure 3d would be obtained. In this case, it would then be possible to get a three-zone SMB exactly equivalent to a four-zone by realizing a two-step process, like the one in Figures 4a and 4b. In practice it is not possible to reach such a point: due to axial dispersion and mass-transfer resistance, dilution occurs and the situation of Figure 3e is reached.

2. The front edge of peak B is established and destroyed during each switching period. Bailly and Tondeur (1992) have shown that the largest entropy production occurs in this precise case. Since the only source of free energy for this entropy production is eluent, its consumption is maximized when compared to the four-zone scheme, in which a constant and smoother concentration gradient exists.

3. There is no theoretical reason why the $T/2$ instant concentration of the raffinate should be representative of the concentration accounted for by the equivalent true countercurrent modelization pattern. Depending on ϵ and K_{raf}, the instant composition of the raffinate could well be zero or $C_{R\ \max}$ at $t = T/2$, where $C_{R\ \max}$ is the less retained component concentration in the plateau region.

Conclusion

We have shown that the equivalent true countercurrent modelization pattern is able to simulate the SMB units with both the four-zone and the three-zone schemes when everything is taken into account.

With respect to the desorbent net consumption, the facts show that the three-zone scheme is unfavorable, even with product splitting. There are both theoretical and practical reasons for which the four-zone scheme is optimal with regard to desorbent requirement.

Literature Cited

Balannec, B., and G. Hotier, *Preparative and Production Scale Chromatography*, Chap. 14, Chromatogr. Sci. Ser., Vol. 61, Marcel Dekker, New York, p. 301 (1992).

Barker, P. E., and G. Ganetos, *Adsorption: Science and Technology*, Kluwer, Dordrecht, The Netherlands, p. 471 (1989).

Barker, P. E., K. England, and G. Vlachogiannis, "Mathematical Model for the Fractionation of Dextran on a Semicontinuous Counter-Current Simulated Moving Bed Chromatrograph," *Chem. Eng. Res. Dev.*, **61**, 241 (1983).

Broughton, D. B., R. W. Neuzil, J. M. Pharis, and C. S. Brearley, "The Parex Process for Recovering Paraxylene," *Chem. Eng. Prog.*, **66**(9), 70 (1970).

Ching, C. B., and D. M. Ruthven, "Experimental Study of a Simulated Counter-Current Adsorption System: I Isothermal Steady State Operation," *Chem. Eng. Sci.*, **40**(6), 877 (1985a).

Ching, C. B., and D. M. Ruthven, "Experimental Study of a Simulated Counter-Current Adsorption System: II Transient Regime," *Chem. Eng. Sci.*, **40**(6), 887 (1985b).

Ching, C. B., K. H. Chu, K. Hidajat, and M. S. Udin, "Comparative Study of Flow Schemes for a Simulated Countercurrent Adsorption Separation Process," *AIChE J.*, **38**, 1744 (1992).

Ching, C. B., C. Ho, and K. Hidajat, "Experimental Study of a Simulated Counter-Current Adsorption System: V. Comparison of Resin and Zeolite Adsorbents for Fructose-Glucose Separation at High Concentration," *Chem. Eng. Sci.*, **42**(11), 2547 (1987).

Ching, C. B., C. Ho, and D. M. Ruthven, "Experimental Study of a Simulated Counter-Current Adsorption System: VI. Nonlinear Systems," *Chem. Eng. Sci.*, **43**(3), 703 (1988).

Ching, C. B., D. M. Ruthven, and K. Hidajat, "Experimental Study of a Simulated Counter-Current Adsorption System: III Sorbex Operation," *Chem. Eng. Sci.*, **40**(8), 1411 (1985).

Ganetsos, G., and P. E. Barker, *Preparative and Production Scale Chromatography*, Chap. 11, Chrom. Sci. Ser., Vol. 61, Marcel Dekker, New York, p. 233 (1992).

Hashimoto, K., M. Yamada, Y. Shirai, and S. Adachi, "Continuous Separation of Glucose-Salts Mixtures with Nonlinear and Linear Adsorption Isotherms by Using Asimulated Moving Bed Adsorber," *J. Chem. Eng. Japan*, **20**(4), 405 (1987).

Hidajat, K., and C. B. Ching, "Simulation of the Performance of a Continuous Counter-Current Adsorption System by the Method of Orthogonal Collocation with Nonlinear and Interacting Adsorption Isotherms," *Trans. Ind. Chem. Eng.*, **68A**, 104 (1990).

Liappis, A. I., and D. W. Rippin, "Simulation of Binary Adsorption in Continuous Countercurrent Operation in Comparison with other Operating Modes," *AIChE J.*, **25**, 455 (1979).

Morbidelli, M., G. Storti, and M. Mazotti, "Operation and Design of a Four-Port Switching Adsorption Separation Unit," *Proc. NSF-CNRS Workshop*, Gif/Yvette, France (1991).

Nicoud, R. M., and M. Bailly, "Choice and Optimization of Operating Modes in Industrial Chromatography," *Proc. Int. Symp. Prep. and Indus. Chromatogr.*, Nancy, France (1992).

Ruthven, D. M., and C. B. Ching, "Counter-Current and Simulated Counter-Current Adsorption Separation Process," *Chem. Eng. Sci.*, **44**(5), 1011 (1989).

Storti, G., M. Masi, S. Carra, and M. Morbidelli, "Modeling and Design of Simulated Moving Bed Adsorption Separation Units," *Prep. Chromatog*, **1**(1), 1 (1988a).

Storti, G., M. Masi, R. Paludetto, M. Morbidelli, and S. Carra, "Adsorption Separation Process: Countercurrent and Simulated Countercurrent Operations," *Comput. Chem. Eng.*, **12**(5), 475 (1988b).

Storti, G., M. Masi, and M. Morbidelli, *Adsorption: Science and Technology*, Kluwer, Dordrecht, The Netherlands, p. 357 (1989a).

Storti, G., M. Masi, S. Carra, and M. Morbidelli, "Optimal Design of Multicomponent Countercurrent Adsorption Separation Process," *Chem. Eng. Sci.*, **44**(6), 1325 (1989b).

Storti, G., M. Mazotti, L. T. Furlan, M. Morbidelli, and S. Carra, "Performance of a Six Port Simulated Moving Bed Pilot Plant for Vapor Phase Adsorption Separation," *Sep. Sci. Tech.*, **27**(14), 1889 (1992).

Tondeur, D., and M. Bailly, *Preparative and Production Scale Chromatography*, Chap. 4, Chrom. Sci. Ser., Vol. 61, Marcel Dekker, New York, p. 79 (1992).

Appendix A

$S = [(1-\epsilon)aL]/T = 3.9\ \mathrm{cm^3/min}$.

Derived zone $I =$ Act. E1 $- [\epsilon/(1-\epsilon)]\ S = 2.3\ \mathrm{cm^3/min}$.

Valid because dextran T_6 recovery is 100%.

A 0.34-$\mathrm{cm^3/min}$ "loss" may not be considered as an unavoidable error. This discrepancy seriously affects the pre-

Table A1. Equivalent to Table 3 in Raffinose 5%-Dextran T6 5% Separation Experiments

Flow Scheme cm^3/min	Four Section		Three Section	
	Actual	Derived	Actual	Derived
Zone I (cm^3/min)	5.5	2.30	5.5	2.3
Zone II (cm^3/min)	4.1	0.90	4.1	0.9
Zone III (cm^3/min)	5.1	1.90	5.1	1.9
Zone IV (cm^3/min)	3.9	0.70	—	—
Makeup desorbent (cm^3/min)	1.6	1.6	5.5	2.3
Feed (cm^3/min)	1.0	1.0	1.0	1.0
Extract (cm^3/min)	1.4	1.4	1.4	1.4
Raffinate (cm^3/min)	1.2	1.2	4.76*	1.56
Switch time/min	10.3	10.3	10.3	10.3
Losses (cm^3/min)	—	—	0.34	0.34

$$*\text{Raffinate} = \frac{\text{feed} \cdot \text{dextran } T_6 \text{ (feed) \%}}{\text{dextran } T_6 \text{ (raffinate) \%}} = 4.76 \text{ cm}^3/\text{min}.$$

dicted concentration profiles, so it may be suspected that dextran T_6 concentration is closer to 1.0 wt. % than to 1.05 wt. %.

Table A2. Equivalent to Table 3 in Raffinose 5%-Fructose 5% Separation Experiments

Flow Scheme cm^3/min	Four Section		Three Section	
	Actual	Derived	Actual	Derived
Zone I (cm^3/min)	9.5	4.4	9.5	4.4
Zone II (cm^3/min)	8.7	3.6	8.7	3.6
Zone III (cm^3/min)	9.2	4.1	9.2	4.1
Zone IV (cm^3/min)	8.4	3.3	—	—
Makeup desorbent (cm^3/min)	1.1	1.1	9.5	2.3
Feed (cm^3/min)	0.5	0.5	0.5	0.5
Extract (cm^3/min)	0.8	0.8	0.8	0.8
Raffinate (cm^3/min)	0.8	0.8	8.7*	3.6
Switch time/min	6.5	6.5	6.5	6.5
Losses (cm^3/min)	—	—	0.50	0.50

$$*\text{Raffinate} = \frac{(\text{feed} \cdot \text{raffinose (feed) \%}) \cdot \text{recovery-(extract} \cdot \text{raffinose (Ext) \%)}}{\text{raffinose (raffinate) \%}} = 8.7 \text{ cm}^3/\text{min}.$$

Appendix B

$S = [(1-\epsilon)aL]/T = 6.2 \text{ cm}^3/\text{min}$.

Derived zone $I = \text{Act. E1} - [\epsilon/(1-\epsilon)]\ S = 4.4 \text{ cm}^3/\text{min}$.

A 0.50-cm^3/min "loss" may not be considered as an unavoidable error. This discrepancy seriously affects the predicted concentration profiles, so it may be suspected that raffinose concentration is closer to 0.245 wt. %/vol than to 0.26 wt. %/vol.

Manuscript received Aug. 25, 1994, and revision received Nov. 8, 1994.